Design and Optimization of a Medium Altitude Long Endurance UAV Wingbox Structure

Y. Naidu[a] and S. Adali[a]

Received 11 October 2013, in revised form 14 May 2014 and accepted 04 June 2014

Abstract This paper describes the design and optimization process of a lightweight Medium Altitude Long Endurance (MALE) Unmanned Aerial Vehicle (UAV) wingbox that has been designed for an aircraft performing Intelligence and Surveillance (ISR) missions. The aircraft wing has been designed and optimized to incorporate a relatively high aspect ratio to decrease drag and extend the flight time. Lightweight isotropic and composite materials have been considered for the design and included in the optimization process. An iterative design method has been used to establish the lightest possible structural mass for the UAV wingbox. The wingbox has been modelled using a finite element analysis for a maximum loading condition of +3.2g. The final optimized wingbox design has been presented in the results section of this paper.

Additional keywords: Wingbox, Unmanned Aerial Vehicle, Lightweight panels, CFRP, honeycomb, sandwich panels

Nomenclature

Roman

b	Wingspan [m]
bdf	Bulk data file
f_t	Flight time [hours]
n	Maximum G-force [m/s]
pcf	pounds per cubic foot
sfc	Specific fuel consumption [l^3/hr.HP]
t_{bf}	Bottom facesheet thickness [mm]
t_c	Core thickness [mm]
t_{tf}	Top facesheet thickness [mm]
AR	Aspect ratio
C_d	Coefficient of drag
C_L	Coefficient of lift
C_r	Root chord [mm]
C_t	Tip Chord [mm]
CUAV	Composite Unmanned Aerial Vehicle
D	Drag Force [N]
F06	SimXpert solution file
FEA	Finite element analysis
H	Height [mm]
HALE	High Altitude Long Endurance
HP	Horsepower
ISR	Intelligence, Surveillance and Reconnaissance
L	Lift Force [N]
LBC	Loading and Boundary Condition
MALE	Medium Altitude Long Endurance
M_e	Empty Mass [kg]
M_f	Fuel Mass [kg]
M_{TO}	Take-off Mass [kg]
Mul	Useful Mass [kg]
MOS	Margin of Safety
S	Wing Area [m^2]
UAV	Unmanned Aerial Vehicle

Greek

λ	Taper Ratio

1 Introduction

The latest designs and innovations in structures and materials have been critical to the improvement of aircraft performance. Lightweight panels and composite materials have allowed designers to lower aircraft structural weight while still maintaining the required stiffness and integrity associated with metallic structures. Improving the weight of an aircraft plays an important role in reducing operating costs, and improving range and efficiency.

The use of composite materials is becoming increasingly predominant in aircraft design. Composite materials offer greater stiffness-to-weight ratios than their metallic counterparts, which have dominated the aircraft structures industry. The Advisory Council for Aerospace Research in Europe (ACARE), have stated that by the year 2020 the carbon dioxide emissions of civil aircraft must be halved when compared to the values recorded in the year 2000[1]. A reduction in aircraft empty mass, made up in a large part by the structural mass, is one of the simplest ways in which aircraft operating efficiency can be improved. Composite materials have been extensively on the Airbus A350, F-22 Raptor and Boeing 787[2-4].

This project can be divided into two main aspects, namely the design of a MALE UAV model and the optimization of the UAV's wingbox structure. The MALE UAV is defined as an aircraft that has no manned crew on board, flying at altitudes between 10 000 and 30 000 feet (or 3048 m and 9144 m), for missions that last ten hours or longer. The baseline aircraft was designed using traditional aeronautical methods and theories, while the structural optimization was carried out using the Hypersizer optimisation software. The design and optimization process has been carried out for several primary structures however this paper focuses on the aircraft wing box structure.

An optimization implies that the design concept will not only meet the set specification, but does so when a target criterion is imposed. In this research project the target was to obtain a minimal structural mass while still maintaining a positive Margin-of-Safety (MOS). This ensured that the lightweight structures would still have the capability to support the aircraft design loads.

2 Objectives

- Design a MALE UAV platform (referred to as the CUAV in this paper) that can be used for ISR missions

- Investigate the suitability of various lightweight panel designs for aircraft wing box panels
- Optimize the aircraft wingbox for the lowest possible mass solution while maintaining a positive MOS

3 Baseline Aircraft

The CUAV was designed based on several MALE UAV aircraft that are already in operation. The Predator (figure 1), Heron and DENEL Seeker 400 were the three aircraft studied for this design project. Adjustments were made for the CUAV mass and mission requirements.

All three of these aircraft are utilised for ISR missions and are all powered by the Rotax 914 engine[5-7]. The MALE UAVs studied for this project are characterised by high AR wings and a slender, narrow fuselage which were adopted for the CUAV. The CUAV adopts the same fuselage shape as the Seeker, in that both share a more rectangular fuselage shape as compared to the traditional circular or elliptical fuselage cross section.

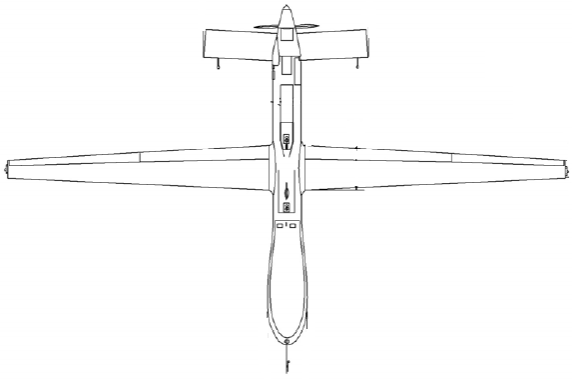

Figure 1 RQ 1BPredator UAV[8]

4 Optimization Process

The initial MALE UAV design was carried out to determine a realistic wing planform size and geometry. The lift distribution and aerodynamic loads were then calculated across the wingspan using theoretical methods. The CUAV wing was created in a 3D CAD modelling package, Autodesk Inventor 2010, from which it was exported in the CATIA format as a parasolid. The parasolid was imported into MSC SimXpert, a FEA program. SimXpert allowed the for the wing loads and constraints to be applied to the model. Hypersizer was unable to create the complex wing loads that were calculated from the wing lift profile.

In order to determine the initial user boundaries that were to be applied to the panel the Hypersizer package was used in its stand \alone mode. Where the optimal layups and thicknesses were obtained through iterative methods. These results were required due to the numerous design and layup concepts available. When considering a composite panel there are several variables that can be optimized, such as ply orientation, layup sequence, material etc. Due to the enormity of these optimization variables the initial optimization step was required to reduce the variables to manageable quantities for the final analysis.

The second level optimization utilised software linking between the FE and the optimization programs. The bulk data file (bdf) and F06 solution files from the FEA package were integrated with Hypersizer to allow for the weight optimization procedure to occur. In this level the final wingbox designs were obtained for both the panels and spar.

The optimized design concept obtained from Hypersizer is primarily based on accurate engineering analyses and secondarily based on discrete optimization techniques[9]. The Hypersizer structural analysis depends on applied and allowable loadings. The allowable loadings are determined as a combination of material strength and the structural design (panel and beam concept, shape, size etc.)[9]. The structural design is controlled by the user whereby the user specified boundary conditions are altered and multiple permutations are analysed before the optimal panel concept is obtained.

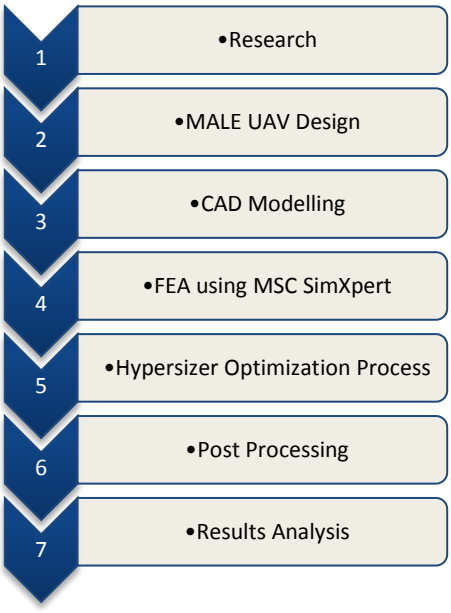

Figure 2 CUAV Design and Optimization Process

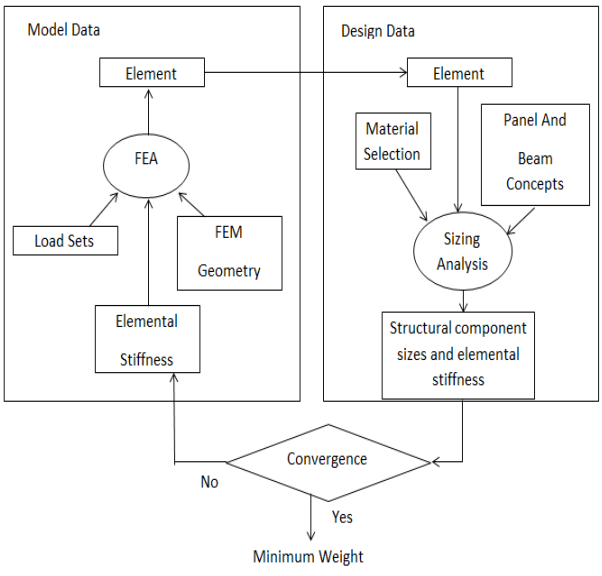

Figure 3 Hypersizer Process[10]

5 Mission Profile

The mission profile is aircraft specific and every mission profile must be created and calculated for that particular aircraft. The mission profile is broken down into the various

stages the aircraft must go through in order to fulfil its primary objectives, in this case that would be to complete ISR missions. There are 6 main stages namely: Taxi (Stage 1), Climb (Stage 2), Cruise (Stage 3), Loiter (Stage 4), Return (Stage 5) and Land, Taxi and Engine Shutdown (Stage 6). The mission profile is illustrated in figure 4.

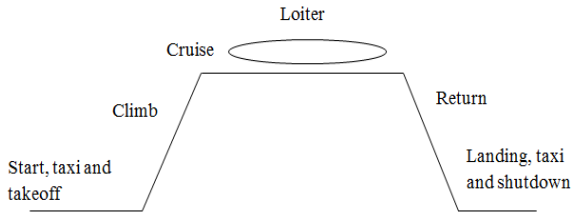

Figure 4 Mission Profile

6 Initial Weight Analysis

The initial weight analysis was required to determine the geometry and sizing specifications of the aircraft. This initial estimate was used as a baseline guide to establish the wing dimensions and planform shape. These initial calculations were then altered based on available data from the baseline aircraft models to suit the CUAV concept and operating capabilities.

The CUAV was designed to carry a useful load of 100 kg; this useful load can be any combination of cameras, sensory equipment or recording devices. By studying the baseline aircraft, namely the Predator and Reaper UAVs, the empty weight ratio was taken to be 0.4. It is important to note that for this aircraft design the empty mass was taken to include the aircraft structure without including the masses for avionics and sensory equipment which were included as a part of the useful aircraft mass.

Table 1 Baseline Aircraft Data[11]

	Predator A	Reaper
Empty Mass	350 kg	1770 kg
Take-off Mass	850 kg	3919 kg
Empty Fraction	0.41	0.45
Wingspan	16.8 m	20.1 m
AR	22	22

The CUAV was designed to use a Rotax piston engine. An average sfc of 0.46 l^3/hr.HP was calculated for the mission flight. An L/D fraction of 22 was selected for use, based on the estimations by Jenkinson and Marchman[12]. Civil aircraft have an L/D value of 17 while modern gliders have an L/D value as high as 40[12]. The CUAV was designed to utilise a slender fuselage and high AR wings thereby giving it a high L/D value. Jenkinson and Marchman[12] estimated a HALE UAV to have an L/D value of 25, being slightly more conservative, the CUAV was estimated to have an L/D value of 22. It was calculated, from equation 1, that the required fuel mass fraction was to be 0.316. An additional ten percent was added to this fraction to allow for any contingencies during the flight and the fuel mass fraction used in the initial weight estimation was taken as 0.347.

$$\frac{M_f}{M_{TO}} = (sfc_{cruise}).\left(\frac{D}{L}\right).(f_t) \quad (1)$$

The initial take-off mass was calculated to be 474 kg, using equation 2. This is comparable to the mass of a light recreational aircraft or a sport glider.

$$M_{TO} = \frac{M_{ul}}{\left[1-\frac{M_f}{M_{TO}}-\frac{M_e}{M_{TO}}\right]} \quad (2)$$

Table 2 CUAV Specifications

Aircraft Specifications	
Wing Span	11.93 m
Wing Area	9.5 m^2
AR	15
Empty Mass	190 kg
Take-off Mass	474 kg
Useful Mass	100 kg
Wing Loading	50 kg/m^2
Rate of Climb	150 m/min
Cruise Speed	21.94 m/s
Ceiling	7620 m/ 25 000 ft
Engine	Rotax 912 Piston Engine

7 Wing Planform

The aircraft wing geometry was designed for a wing loading of 50 kg/m^2, which is comparable to the wing loading of the Cessna 152 light aircraft[13]. The CUAV will not be subjected to high g manoeuvres and turns during flight and as such a more modest wing loading was chosen for the design of the aircraft wing. Using the wing loading of 50 kg/m2 resulted in a calculated wing span of 11.93 m and a wing area of 9.5 m^2.

An effect of increasing the wing taper ratio is that the lift at the wing tips also increases, therefore a wing taper ratio of 0.4 was chosen for the CUAV. This taper ratio is slightly less than that used by the baseline MALE UAV's, the Predator UAV uses a taper ratio of 0.36[8]. The CUAV was designed to fly ISR missions which entail long flights and so the wing has been designed to minimize the drag and maximise the lift to obtain a high L/D ratio.

The wing has been designed to utilise a high aspect ratio. The use of a higher AR wing will allow for a reduction in drag while providing the equivalent lift force of a thicker wing. In a conventional metal wing structure the use of high AR wings will require the addition of internal reinforcements to prevent wing failure[1]. The additional structural reinforcements result in a heavier wing which lowers the payload carrying capacity of the aircraft. However with the use of a composite wing the materials can be tailored so that the layup is created to deal with the specific loading conditions of the wing. A higher AR wing will also allow for a small chord length to be used and this will motivate laminar flow over a larger portion of the aircraft wing surface.

Table 3 Wing Planform Specifications

Wing Geometry	
$^b/_2$	5960 mm
C_r	1136 mm
C_t	455 mm
Taper Ratio	0.4
Aspect Ratio	15

The NACA 4412 profile was chosen for the wing. This provided a high C_L with a C_L Max = 1.67. The high camber

of the profile also gave the wing a milder stalling characteristic and reduced the C_d at lower speeds.

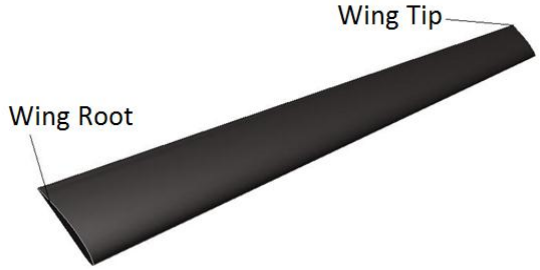

Figure 5 MALE UAV Port-side wing

Figure 6 NACA 4412 Airfoil

8 Aerodynamic Loading

The lift distribution across a trapezoidal wing differs across the wing span. At the root the lift is the highest while the lift is subsequently reduced at the wing tip. The wing loading analysis was performed taking into account three major load conditions, namely lift, fuel load and the actual structural mass of the wing. The lift analysis was performed for a gust positive vertical load factor of +3.2g, which is the maximum wing loading that the aircraft will experience during its mission.

The lift distribution of the wing was calculated by using Shenk's Approximation[12]. The approximation assumes that the lift distribution long the wingspan is the average of the lift based on a trapezoidal wing (equation 3) and the lift based on an elliptical wing (equation 4)[11].

Trapezoidal lift:

$$L(y) = \frac{2L}{b(1+\lambda)}\left[1 - \frac{2y}{b}(1-\lambda)\right] \quad (3)$$

Elliptical lift:

$$L(y) = \frac{4L}{\pi b}\sqrt{1 - \left(\frac{2y}{b}\right)^2} \quad (4)$$

To determine the lift distribution the aircraft wing was divided into eleven panels. Each panel had a span of 548.6 mm, excluding the eleventh panel located at the wingtip which had a span of 478.5 mm. The chord length of each panel was calculated from equation 5. A panel by panel analysis was required to determine the loading cases at each of the panel midpoints located along the wingspan.

$$c(y) = \frac{2S}{b(1+\lambda)}.\left[1 - \left(\frac{2y}{b}\right)(1-\lambda)\right] \quad (5)$$

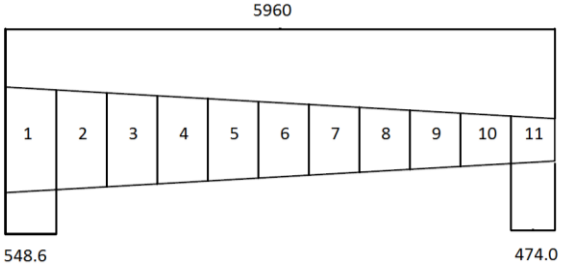

Figure 7 Wing Panels

Table 4 Wing Lift Distribution

Panel Number	Panel Midpoint (m)	Trapezoi-dal Lift (kg/m)	Elliptical Lift (kg/m)	Average Lift (kg/m)
1	0.274	176	161	168.5
2	0.823	166	160	163
3	1.372	156	157	156.5
4	1.920	146	153	149.5
5	2.469	136	147	141.5
6	3.018	126	139	132.5
7	3.566	116	129	122.5
8	4.115	106	117	111.5
9	4.663	96	101	98.5
10	5.212	86	78	82
11	5.726	77	45	61
Wing Tip	5.965	72	3	37.5

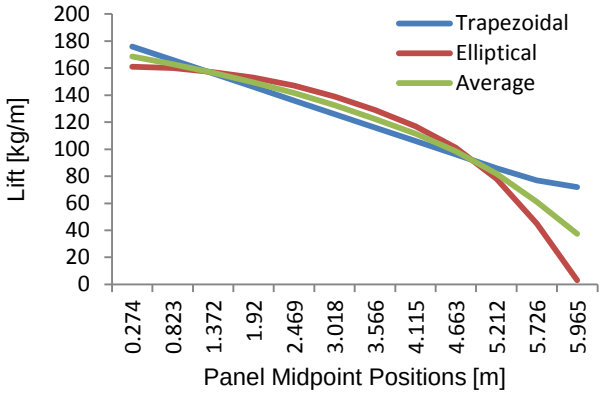

Figure 8 Lift Distribution

9 Wing Panel Concepts

Two panel concepts were investigated for the optimization process, namely stiffened (isogrid, orthogrid and waffle) and unstiffened panels (honeycomb and foam sandwich). Honeycomb panels have been extensively used in the composites industry for their high stiffness to mass ratio. The isogrid concept has been investigated using both isotropic and composite materials in order to establish mass savings by using orthotropic composite materials in place of traditional light weight, isotropic materials.

10 FEA Setup

The 3D wing model was created in Autodesk Inventor. Thereafter the model was imported as a parasolid into MSC SimXpert. The finite element package was required to set up the wing loading condition as well as applying constraints to the wing model.

The wing was fixed at the root using the fixed LBC, as it would be if it were attached to the fuselage of the aircraft. The wing tip was allowed to experience six degrees of freedom. This allowed the wing to be constrained in the way it would be on a static testing rig. The lift and fuel loads were applied along the wing span, as per Shenk's Approximation. A linear static analysis was used for the solution case. This was deemed suitable as the wing would be exposed to the highest loading conditions that it would experience and no dynamic testing was applied at this stage. Figures 9 and 10 depict the wingbox and spar respectively,

with the LBC's indicated as green arrows for the fixed constraint and red arrows for the applied loads.

The wing spar was created using 1D CBAR elements in SimXpert. The nodes on the spar were attached to the panel skin by RBE2 rigid body elements. The wingbox panels were meshed using CQUAD4 elements. Due the relatively small skin thickness, when compared to the panel length, it was deemed suitable to use shell elements to model the wing skin[14].

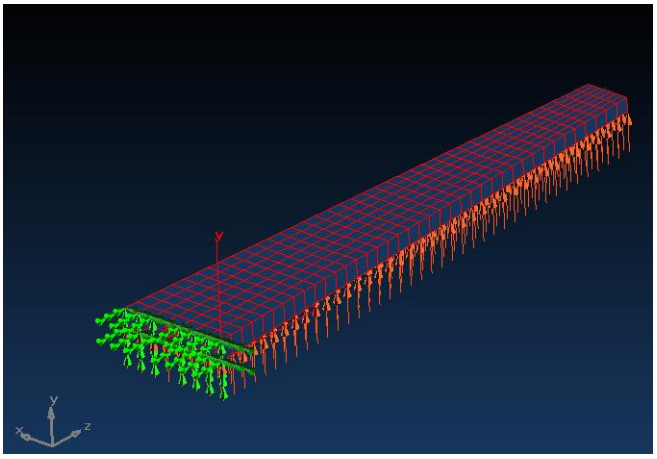

Figure 9 Wing Finite Element Model with LBC's

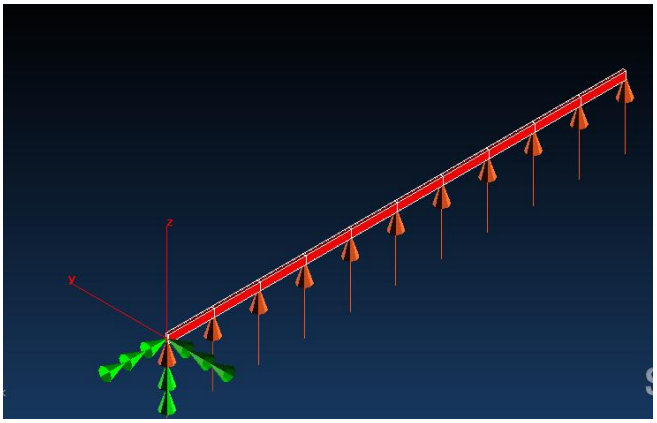

Figure 10 Wing Spar (Wingbox skin removed)

11 Optimization results

Hypersizer bases the panel geometry on the component defined in the FEA, where the component is defined as the smallest sizing variable that Hypersizer will optimize[15]. Initial attempts to optimize the entire wing box as a single component resulted in an excessively heavy design. This was due to the highest stress being present at the wing root, while the stress decreased along the wingspan from the root to the tip. This method was unfavourable towards the overall aim of achieving the lowest possible wing box mass. Three sections of the wing were then identified for optimization, namely: wing root, wing midpoint and the wing tip. This allowed for a reduction in panel dimensions with a decrease in panel load. This method also enabled the use of ply drops along the wing to reduce the overall facesheet thickness for the unstiffened panel concepts. The lightest orthotropic stiffened panel design has been presented in the results section but it is important to note that the panel design was evaluated with several titanium and steel alloys as well. However these are far heavier and have been neglected from the results presented in this paper.

12 Mass Analysis

12.1 Panel Geometry

The panel was designed using a Hexcel, honeycomb core and graphite-epoxy facesheets. The greatest panel height was attributed to the core section – which had a comparably lower density than the graphite-epoxy facesheets.

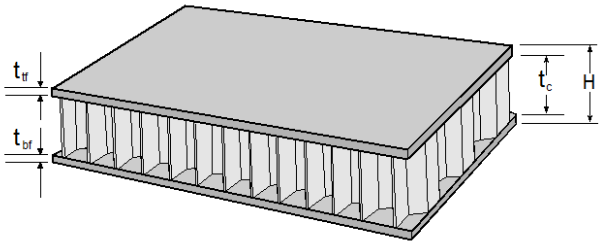

	Wing Section 1	Wing Section 2	Wing Section 3
t_{tf} (mm)	1.40	0.70	0.70
t_{bf} (mm)	1.40	0.70	0.70
t_c (mm)	75	30	20
H (mm)	77.80	31.40	21.40

Figure 11 Honeycomb Panel Geometry [Hypersizer Diagram]

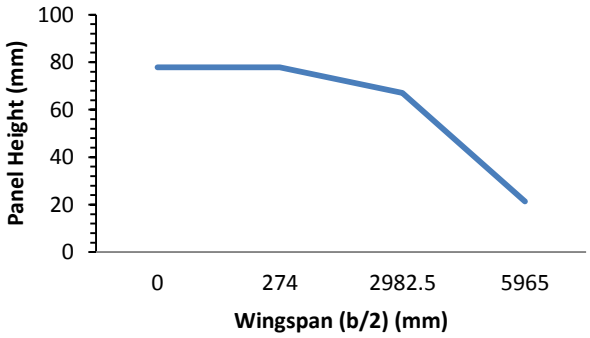

Figure 12 Panel Height vs. Span

12.2 Beam Geometry

The wingbox was designed to incorporate an I-beam wing spar (figure 13). This beam was able to provide the greatest beam stiffness and strength while still having the lightest weight. Each of the beam dimensions was used as a sizing variable to obtain the lowest possible beam mass.

13 Discussion

The sandwich panel designs demonstrated the lowest wing box mass within the acceptable safety limits. As expected the greatest panel thickness and mass was located at the wing root, which experienced the greatest loading and resultant stress. The use of ply drops allowed for the large reduction in panel height across the span. This allowed for a unique structural solution to be obtained at each of the three wing locations (root, midpoint and tip).

Graphite epoxy has proven to be the material of choice when obtaining a low mass design and has been used for

both the wing panels and spar. The high stiffness-to-weight ratio of this orthotropic material has allowed for it to be used in structures that would have been previously produced using metallic components with a far greater mass.

The composite I beam demonstrated a far lower structural mass than any of the other beam concepts (rectangular, channel and tubular beams). The ability to control the boundary conditions as well as the use of material linking has allowed for a beam solution to be created where the top and bottom flange widths are independent of each other. This has allowed for a large reduction in bottom flange width when compared to the upper flange and has resulted in a large weight saving.

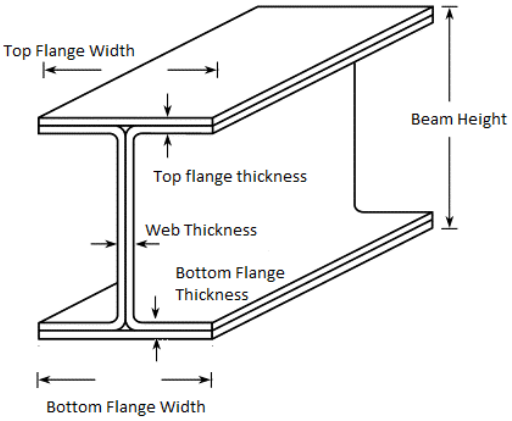

Beam Geometry	
Web Thickness (mm)	6
Beam Height (mm)	200
Bottom Flange Width (mm)	17.5
Bottom Flange Thickness (mm)	6
Top Flange Width (mm)	50
Top Flange Thickness (mm)	6

Figure 13 I Beam Diagram[16]

14 Conclusion

A MALE UAV model, namely the CUAV, has been designed for ISR missions. This baseline model has had its wingbox optimized using the Hypersizer code. The MALE UAV wing was optimized using several panel concepts using a variety of orthotropic and isotropic materials. The sandwich panel designs have demonstrated the lowest masses while still providing a positive safety factor for the aircraft. A composite I beam spar has also been designed for use in the CUAV. The entire wing has incorporated graphite epoxy in its structure with aluminium only being present in the honeycomb core. While isotropic materials may have been used in the majority of previous aircraft designs they have been proven to be outdated in terms of mass sensitivity.

References

1. *Edwards T*, Composite Materials Development Under the NGCW Research Program, *http://www.atkinsglobal.com/~/media/Files/A/Atkins-Global/Attachments/sectors/aerospace/library-docs/technical-papers/ngcw-research.pdf*, 1 Jul 2014.
2. *Guizzo E*, Winner Carbon Takeoff, IEEE Spectrum, January 2006, *http://spectrum.ieee.org/aerospace/aviation/winner-carbon-takeoff*, 1 Jul 2014.
3. *Marsh G*, Aircraft Wing Worker for the World, *Reinforced Plastics*, May/June 2010.
4. *Park Y-B, Nguyen K-H, Kweon J-H, Choi J-H, Han J-S*, Structural Analysis of a Composite Target-drone, *International Journal of Aeronautical and Space Sciences*, 12, 1, 84-91, 2011.
5. IAI Heron Factsheet, *http://www.israeli-weapons.com/weapons/aircraft/uav/heron/Heron.html*, 15 Dec 2011.
6. MQ-1B Predator Factsheet, *www.af.mil/information/factsheets/factsheet.asp?id=122*, 7 Jan 2012.
7. MQ-9 REAPER Factsheet, *www.af.mil/information/factsheets/factsheet.asp?fsID=6405*, 7 Jan 2012.
8. *Martin LC*, Airfield Planning and Design, Criteria for Unmanned Aircraft Systems (UAS), Engineering Technical Letter (ETL) 09-1, Department of the Air force, 2009.
9. *Collier C, Yarrington P and Pickenheim M*, The HyperSizing Method for Structures, *NAFEMS World Congress*, Newport, Rhode Island, Apr 25-28, 1999.
10. *Collier C*, An Integrated FEA and Design Optimization System for Composite Structures, *MSC World Users' Conference*, Newport Beach, CA, June 1996.
11. *Nicolai LM and Carichner GE*, Fundamentals of Aircraft and Airship Design, *AIAA Education Series*, Virginia, USA, 2010.
12. *Jenkinson LR and Marchman J*, Aircraft Design Projects: for Engineering Students, American Institute of Aeronautics and Astronautics, Inc, 2003.
13. *Frawley G*, The Cessna 150 and 152, The International Directory of Civil Aircraft, *www.airliners.net/aircraft-data/stats.main?id=138*, 20 Dec 2011.
14. MSC SimXpert - Workspace User's Guides Structures Workspace Guide, User Manual.
15. *Collier C*, Hypersizer Pro User Manual, Edition 5.3.
16. *Attia O, Kinloch AJ, Mathews FL*, Modelling the Fatigue Life of Polymer–matrix Fibre-composite Components, *Composite Science and Technology*, 61, 15, 2273-2283, 2001.

Appendix A – Detailed Results

Composite I Beam

Table 5 Beam Geometry

Web thickness (mm)	6
Beam height (mm)	200
Bottom flange width (mm)	17.5
Bottom flange thickness (mm)	6
Top flange width (mm)	50
Top flange thickness (mm)	6

Table 6 Results

Material	Graphite/Epoxy AS4 3502/Tape
Length	5.897 m
Per unit mass	2.42 kg/m
Component mass	14.27 kg
Margin of safety	0.0127
Failure mode	Crippling Failure

Wing Section 1

Table 7 Panel Geometry

Core thickness	62.5 mm
Top face thickness	2.096 mm
Bottom face thickness	2.515 mm
Panel height	67.11 mm
No. of plies (Top face)	10
No. of plies (Bottom face)	12
Layup Top Face	[45/ -45/ 45/ -45/ 0]
Layup Bottom Face	[45/ -45/ 45/ -45/ 0/ 0]

Table 8 Results

Core material	Hexcel 6.1 pcf 1/8-5052-0.0015
Facesheet material	Graphite/Epoxy AS4/3501 Form: Fabric
Area	2.795 m^2
Per unit mass	13.36 kg/m^2
Component mass	37.35 kg
Margin of safety	0.1532
Failure mode	Tensile failure in top honeycomb face

Wing Section 2

Table 9 Panel Geometry

Core thickness	30 mm
Top face thickness	0.6985 mm
Bottom face thickness	0.6985 mm
Panel height	67.11 mm
No. of plies (Top face)	10
No. of plies (Bottom face)	10
Layup Top Face	[0/45/90/-45/0]s
Layup Bottom Face	[0/45/90/-45/0]s

Table 10 Results

Core material	Hexcel 6.1 pcf 1/8-5052-0.0015
Facesheet material	Graphite/Epoxy AS4/3501 (Fabric)
Area	2.24 m^2
Per unit mass	5.13 kg/m^2
Component mass	11.5 kg
Margin of safety	0.0047
Failure mode	Tensile failure in the bottom honeycomb face

Wing Section 3

Table 11 Panel Geometry

Core thickness	20 mm
Top face thickness	0.6985 mm
Bottom face thickness	0.6985 mm
Panel height	21.4 mm
No. of plies (Top face)	5
No. of plies (Bottom face)	5
Layup Top Face	[-45/45/-45/45/0]s
Layup Bottom Face	[-45/45/-45/45/0]s

Table 12 Results

Core material	Hexcel 6.1 pcf 1/8-5052-0.0015
Facesheet material	Graphite/Epoxy AS4/3501 (Fabric)
Area	1.47 m^2
Per unit mass	4.15 kg/m^2
Component mass	6.10 kg
Margin of safety	0.1623
Failure mode	Tsai-Wu failure criterion in top honeycomb face

Appendix B – Materials

Hexcel 6.1 pcf (97.43 kg/m^3) 1/8-5052-.0015

Density: 97.4336 (kg/m^3)

Table 13 Properties

Tension *Et (GPa)	1.65
Compression *Ec (GPa)	1.65
Shear (Transverse) *Gw (GPa)	0.28
Shear (Longitudinal) *Gl (GPa)	0.68
Tension (MPa)	4.69
Shear (Transverse) (MPa)	1.88
Shear (Longitudinal) (MPa)	3.14
Crush (MPa)	3.10

Graphite/Epoxy AS4/3501-6 Fabric

Form: Fabric

Density: 1577.76 (kg/m^3)

Table 14 Stiffness

Tension	0°, *Et1	(GPa)	67.57
Tension	90°, *Et2	(GPa)	67.57
Tension	Poisson's Ratio, *vt12		0.04
Compression	0°, *Ec1	(GPa)	63.43
Compression	90°, *Ec2	(GPa)	63.434
Compression	Poisson's Ratio, *vc12		0.04
Shear	In-Plane, *G12	(GPa)	3.544
Shear	Interlaminar, G13	(GPa)	3.54
Shear	Interlaminar, G23	(GPa)	3.54

Table 15 Stress Allowables

In-Plane Tension	0°, *Ftu1	(MPa)	806.72
In-Plane Tension	90°, *Ftu2	(MPa)	806.72
In-Plane Compression	0°, *Fcu1	(MPa)	792.925
In-Plane Compression	90°, *Fcu2	(MPa)	792.93
In-Plane Shear,	*Fsu12	(MPa)	97.909
Out-of-Plane	Interlaminar, Fsu13	(MPa)	66.88
Out-of-Plane	Interlaminar, Fsu23	(MPa)	36.54

Table 16 Strain Allowables

In-Plane Tension	0°, *etu1	(μm/m)	11938.78
In-Plane Tension	90°, *etu2	(μm/m)	11938.78
In-Plane Compression	0°, *ecu1	(μm/m)	12500
In-Plane Compression	90°, *ecu2	(μm/m)	12500
Shear	In-Plane, *esu12	(μm/m)	27626.46

Graphite/Epoxy AS4/3502 Tape

Form: Tape

Density: 1577.76 (kg/m^3)

Table 17 Stiffness

Tension	0°, *Et1	(GPa)	133.07
Tension	90°, *Et2	(GPa)	9.3
Tension	Poisson's Ratio, *vt12		0.34
Compression	0°, *Ec1	(GPa)	124.11
Compression	90°, *Ec2	(GPa)	9.72
Compression	Poisson's Ratio, *vc12		0.34
Shear	In-Plane, *G12	(GPa)	3.74
Shear	Interlaminar, G13	(GPa)	3.74
Shear	Interlaminar, G23	(GPa)	3.74

Table 18 Stress Allowables

In-Plane Tension	0°, *Ftu1	(MPa)	1413.48
In-Plane Tension	90°, *Ftu2	(MPa)	148.93
In-Plane Compression	0°, *Fcu1	(MPa)	1179.05
In-Plane Compression	90°, *Fcu2	(MPa)	116.66
Shear	In-Plane, *Fsu12	(MPa)	92.393
Out-of-Plane	Interlaminar, Fsu13	(MPa)	55.99
Out-of-Plane	Interlaminar, Fsu23	(MPa)	36.54

Table 19 Strain Allowables

In-Plane Tension	0°, *etu1	(μm/m)	10621.76
In-Plane Tension	90°, *etu2	(μm/m)	16000
In-Plane Compression	0°, *ecu1	(μm/m)	9500
In-Plane Compression	90°, *ecu2	(μm/m)	12000
Shear	In-Plane, *esu12	(μm/m)	24677.72